Effect of compositional variations on electrical properties in phase switching (Pb,La)(Zr,Ti,Sn)O_3 thin and thick films

BAOMIN XU*, YAOHONG YE, QING-MING WANG, N. G. PAI, L. E. CROSS
Materials Research Laboratory, Pennsylvania State University, University Park, Pennsylvania 16802, USA
E-mail: bxx2@psu.edu

The composition-dependent electrical properties in (Pb,La)(Zr,Ti,Sn)O_3 antiferroelectric-ferroelectric phase switching thin and thick films have been systematically studied and compared with bulk ceramics. The films were deposited on Pt-buffered silicon substrates by a sol-gel method. The results show that the dependence of low-field dielectric properties on compositions in the films is similar to that in bulk ceramics but the variation of high field properties (polarization or hysteresis loops) is quite different, which may be attributed to the special mechanical boundary condition of the films. While all the films with compositions in the antiferroelectric tetragonal region in the phase diagram demonstrate the existence of remanent polarization in the hysteresis loops, the films with zero remanent polarization can be obtained in the antiferroelectric orthorhombic region. This is because the films are under high tensile stress due to the thermal mismatch between the film and substrate, which tends to stabilize the ferroelectric phase and causes the retention of ferroelectric phase for the films in the antiferroelectric tetragonal region because of their relatively small free energy difference between the antiferroelectric phase and ferroelectric phase.

1. Introduction

Antiferroelectric-to-ferroelectric phase switching ceramics in lead zirconate titanate stannate family have been extensively studied since 1960s for energy storage capacitor and high strain actuator/transducer applications [1–6]. In these ceramics, the free energy difference between the antiferroelectric (AFE) phase and ferroelectric (FE) phase can be modified to such an extent that a phase switching between the AFE and FE phases can be realized by applying an electrical field. This field-induced phase switching is accompanied with a volume expansion due to the larger primitive cell of the FE phase, hence large strains can be expected to be concurrent with the phase switching [3]. In fact, the phase switching strain can be 3 to 4 times larger than the strain level in conventional piezoelectric ceramics [5, 6]. On the other hand, a large amount of charge can be stored in the FE phase because the dipoles transfer from the antiparallel state in the AFE phase to the parallel state in the FE phase. These stored charges will be released upon switching back to the AFE phase after electrical field removal; thus very high instantaneous current can be supplied [1]. Depending on composition and temperature, the AFE-to-FE phase switching can occur as a step function of electrical field, or can change gradually with electrical field. These two types of switching are characterized by "square" and "slanted" hysteresis loops, which allow for digital or analog mechanical motion [3]. However, for energy storage applications, materials with square hysteresis loops are preferred [1].

In 1964 Berlincourt reported the phase diagrams of the lead niobium zirconate titanate stannate system and the lead lanthanum zirconate titanate stannate ((Pb,La)(Zr,Ti,Sn)O_3) system [3]. Shown in Fig. 1 is the phase diagram of the $Pb_{0.97}La_{0.02}$(Zr,Ti,Sn)O_3 system. It mainly consists of an AFE orthorhombic region (AFE_O), AFE tetragonal region (AFE_T), low temperature FE rhombohedral region ($FE_{R(LT)}$), as well as high temperature ferroelectric rhombohedral region ($FE_{R(HT)}$) and ferroelectric tetragonal region (FE_T). For bulk ceramics most of the compositions are chosen in the AFE_T region close to the AFE_T-$FE_{R(LT)}$ phase boundary. This is because the switching fields for the compositions in the AFE_O region are so high that they may be higher than the dielectric breakdown strength of the bulk ceramics.

Studies on AFE thin (film thickness <1 μm) and thick (film thickness >1 μm) films in lead zirconate titanate stannate family have been reported by several groups, for microactuator applications in microelectromechanical systems (MEMS) [7–9] and decoupling capacitors in advanced multichip modules (MCMs)

* Author to whom all correspondence should be addressed.

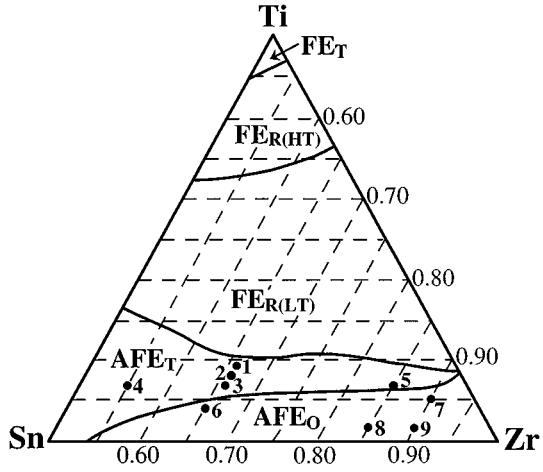

Figure 1 $Pb_{0.97}La_{0.02}(Zr,Ti,Sn)O_3$ phase diagram and the compositions used in this work.

[10, 11]. However, most of the films have some remanent polarization in the hysteresis loops, which is believed to be due to the retention of the FE phase [9]. The compositions for most of these films are still in the AFE_T region as that described for bulk ceramics [8], but some compositions are in the AFE_O region with low Zr contents and close to the AFE_T-AFE_O phase boundary [7, 9].

To fully diminish the remanent polarization or the retention of ferroelectric phase is important for AFE films because the retention of ferroelectric phase will decrease the strain level induced by the phase switching and the energy storage density (the energy storage density is equal to the area between the polarization axis and the back arm of the hysteresis loop [1]). Our recent work demonstrates that the AFE thin and thick films with zero remanent polarization and square hysteresis loops can be obtained when the compositions are chosen in the AFE_O region with high Zr contents [10–12]. Moreover, these AFE films can have a very fast charge release speed in the nanosecond range and develop strain levels more than 0.4%, which are very attractive for high speed decoupling capacitor and microactuator applications [13, 14].

Although a lot of work have been done on the preparation and characterization of AFE films, a systematic study on the composition dependence of electrical properties has not been reported, especially for the compositions in the AFE_O region which are seldom studied even for bulk ceramics. Since thin films offer the advantages of high dielectric strength and low operation voltage, AFE films with compositions in the AFE_O region should be practical for applications. In this work, we attempt to pin down the composition–property relationship in the AFE-FE phase switching thin and thick films in $(Pb,La)(Zr,Ti,Sn)O_3$ system, with the compositions both in the AFE_T region and in the AFE_O region. Both the weak field dielectric properties and the high field properties (field-induced polarization or hysteresis loops) are reported and compared with bulk ceramics.

2. Experimental procedure

The various compositions used in this work are given in Table I and their positions in the phase diagram are shown in Fig. 1. The substrate used is an n-type (100) oriented Si wafer with 0.5 μm-thick thermally grown SiO_2 layer, 0.02 μm-thick sputtered Ti adhesion layer, and 0.15 μm-thick Pt bottom electrode. The thin films are prepared from 2-methoxyethanol based sol-gel method, with the film thickness around 0.4 μm. By using a multi-step annealing process and multiple PbO overcoat layers, thick films, with the thickness of about 5 μm are prepared from acetic acid based sol-gel method. The flow chart to make the thin films is given in Fig. 2. Lead acetylacetonate, titanium isopropoxide, zirconium *n*-propoxide, tin acetate, and lanthanum ethoxide were added to 2-methoxyethanol and the mixture was refluxed at 115°C for 12 hours. The solution was then cooled to room temperature and 4% formamide was added to promote proper drying and to adjust the concentration to be 0.4 M. The flow chart to make thick films is shown in Fig. 3. Lead acetate trihydrate, tin acetate and lanthanum ethoxide were initially dissolved in acetic acid and the mixture was distilled at 150°C to remove the associated water. After cooling down, zirconium *n*-propoxide and titanium

TABLE I The studied films and their compositions

Designation	Composition	Phase	Film type
Thin-1	$Pb_{0.97}La_{0.02}(Zr_{0.66}Ti_{0.09}Sn_{0.25})O_3$ (PLZTS 2/66/9/25)*	AFE tetragonal	Thin film
Thin-2	$Pb_{0.97}La_{0.02}(Zr_{0.66}Ti_{0.08}Sn_{0.26})O_3$ (PLZTS 2/66/8/26)	AFE tetragonal	Thin film
Thin-3	$Pb_{0.97}La_{0.02}(Zr_{0.66}Ti_{0.07}Sn_{0.27})O_3$ (PLZTS 2/66/7/27)	AFE tetragonal	Thin film
Thin-4	$Pb_{0.97}La_{0.02}(Zr_{0.55}Ti_{0.07}Sn_{0.38})O_3$ (PLZTS 2/55/7/38)	AFE tetragonal	Thin film
Thin-5	$Pb_{0.97}La_{0.02}(Zr_{0.85}Ti_{0.07}Sn_{0.08})O_3$ (PLZTS 2/85/7/8)	AFE tetragonal	Thin film
Thin-6	$Pb_{0.97}La_{0.02}(Zr_{0.65}Ti_{0.04}Sn_{0.31})O_3$ (PLZTS 2/65/4/31)	AFE orthorhombic	Thin film
Thin-7	$Pb_{0.97}La_{0.02}(Zr_{0.90}Ti_{0.05}Sn_{0.05})O_3$ (PLZTS 2/90/5/5)	AFE orthorhombic	Thin film
Thin-8	$Pb_{0.97}La_{0.02}(Zr_{0.85}Ti_{0.02}Sn_{0.13})O_3$ (PLZTS 2/85/2/13)	AFE orthorhombic	Thin film
Thin-9	$Pb_{0.97}La_{0.02}(Zr_{0.90}Ti_{0.02}Sn_{0.08})O_3$ (PLZTS 2/90/2/8)	AFE orthorhombic	Thin film
Thick-3	$Pb_{0.97}La_{0.02}(Zr_{0.66}Ti_{0.07}Sn_{0.27})O_3$ (PLZTS 2/66/7/27)	AFE tetragonal	Thick film
Thick-6	$Pb_{0.97}La_{0.02}(Zr_{0.65}Ti_{0.04}Sn_{0.31})O_3$ (PLZTS 2/65/4/31)	AFE orthorhombic	Thick film
Thick-9	$Pb_{0.97}La_{0.02}(Zr_{0.90}Ti_{0.02}Sn_{0.08})O_3$ (PLZTS 2/90/2/8)	AFE orthorhombic	Thick film

*The formula in the brackets is the abbreviation of the composition.

ΔThe dotted line is used to separate the thin film samples in AFE tetragonal region, the thin film samples in AFE orthorhombic region, and the thick film samples.

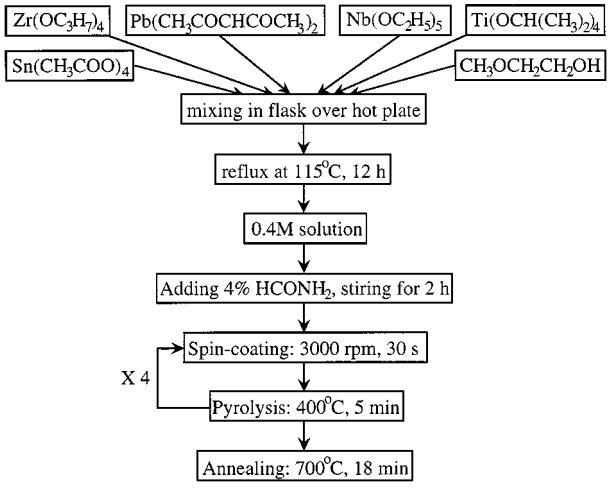

Figure 2 Flow chart to prepare AFE thin films using 2-methoxyethanol based sol-gel method.

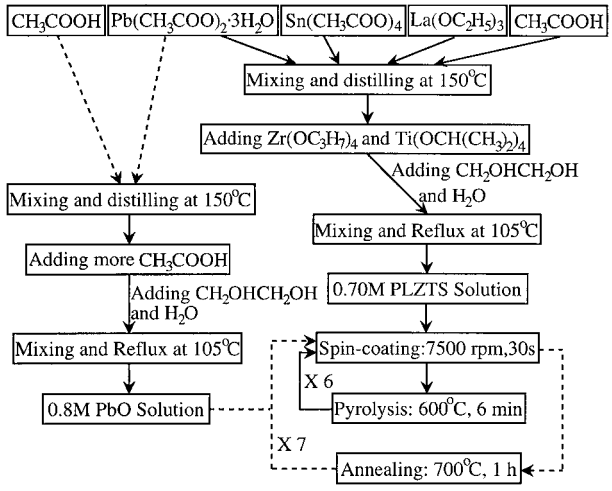

Figure 3 Flow chart to prepare AFE thick films using acetic acid based sol-gel method.

isopropoxide were added and then the solution was refluxed at 105°C for 1 hour. Ethylene glycol and deionized water were added during reflux to control the viscosity and to adjust the concentration to be 0.70 M (the final solutions are simply called as PLZTS solutions). The 0.8 M PbO overcoat solution was prepared using the similar procedure.

The thin films were deposited through a simple multi-step spin-on procedure. The films were pyrolyzed at 400°C for 5 minutes on a hot plate after the deposition of each layer and annealed at 700°C for 18 minutes after the 4th layer deposition. The procedure to deposit thick films is more complicated, which we termed as multi-step annealing with multiple PbO overcoat layers. The films were first pyrolyzed at 600°C for 6 minutes after the deposition of each layer, then they were covered with PbO overcoat solution and annealed at 700°C for 1 hour after the deposition of every 6 PLZTS layers. This cycle was repeated until 42 layers of PLZTS solution were coated. This is because in thick films, much longer time will be spent for the perovskite phase (which nucleates at the film/electrode interface) to grow through the films and reach film surface, thus allowing more time for lead evaporation and requiring more PbO at the film surface for compensation. Using PbO overcoat layers and multi-step annealing procedure is necessary to obtain pure perovskite phase and dense surface microstructure. Details on the effects of multi-step annealing and PbO overcoat layers are beyond the scope of this paper and can be found in Ref. 12.

Crystallization of the films after annealing was examined by a Scintag X-ray diffractometer (XDS 2000, Scintag) using Cu K_α radiation ($\lambda = 1.5418$ Å). The XRD patterns were recorded at a rate of 2°/min with the 2θ range from 20° to 60°. Microstructure of the films was studied using a scanning electron microscope (DS 130, Kevex Instruments, CA). The film thickness was measured by a surface profilometer (Alpha-step 500, Tencor Instruments, NH), with the films partially etched by using the HF-HNO_3 solution. In order to measure the electrical properties, platinum top electrodes with a diameter of 1.6 mm were deposited by a sputtering method. The low field dielectric properties were measured using an HP 4274A LCR meter with an oscillating field of about 10 mV/μm. The P-E hysteresis loops (field-induced polarization) were measured using a modified Sawyer-Tower circuit with a 50 Hz, triangular waveform driving signal. All the measurements were conducted at room temperature.

3. Results

All the films are shown to be a single-phase perovskite structure by the X-ray diffraction (XRD) analyses. The XRD patterns of some films are given in Fig. 4. The

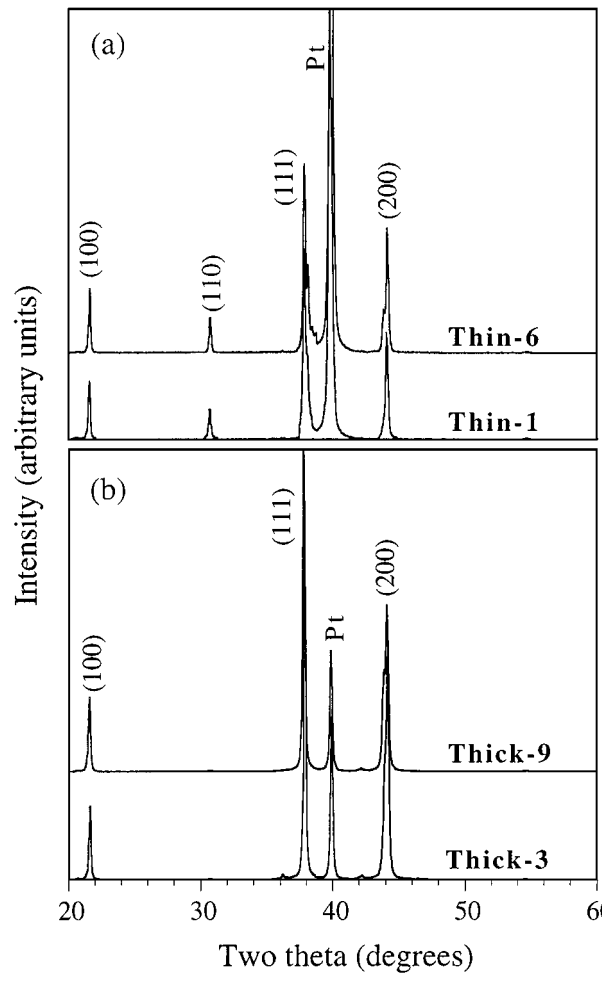

Figure 4 X-ray diffraction patterns of some samples. (a) Thin films samples; (b) Thick films samples.

TABLE II Electrical properties of the films

Designation	Thickness (μm)	ε_r at 1 kHz	tan δ (%)	$E_{AFE\rightarrow FE}$ (kV/cm)	$E_{FE\rightarrow AFE}$ (kV/cm)	P_{MAX} ($\mu C/cm^2$)
Thin-1	0.40	815	3.5	80	39	47.5
Thin-2	0.42	630	2.5	108	54	43.0
Thin-3	0.42	540	2.8	134	65	40.5
Thin-4	0.40	675	2.7	138	73	41.0
Thin-5	0.38	385	2.6	145	48	42.5
Thin-6	0.43	437	2.8	195	176	35.0
Thin-7	0.44	269	2.7	225	132	40.5
Thin-8	0.42	240	2.2	232	178	38.0
Thin-9	0.40	232	2.0	235	170	40.0
Thick-3	4.95	585	2.9	138	71	44.5
Thick-6	5.07	446	2.0	198	182	40.5
Thick-9	5.10	235	2.1	256	184	45.0

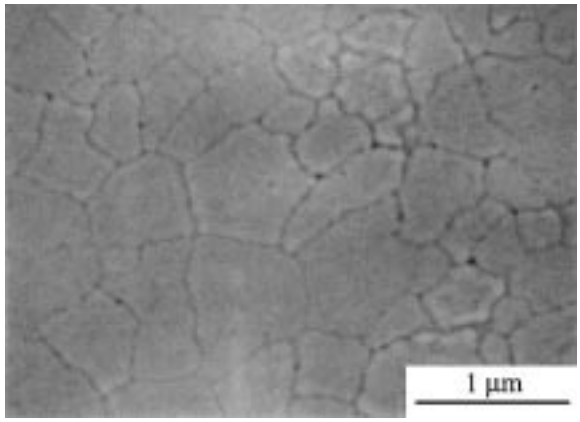

Figure 5 SEM microstructure of sample Thin-8.

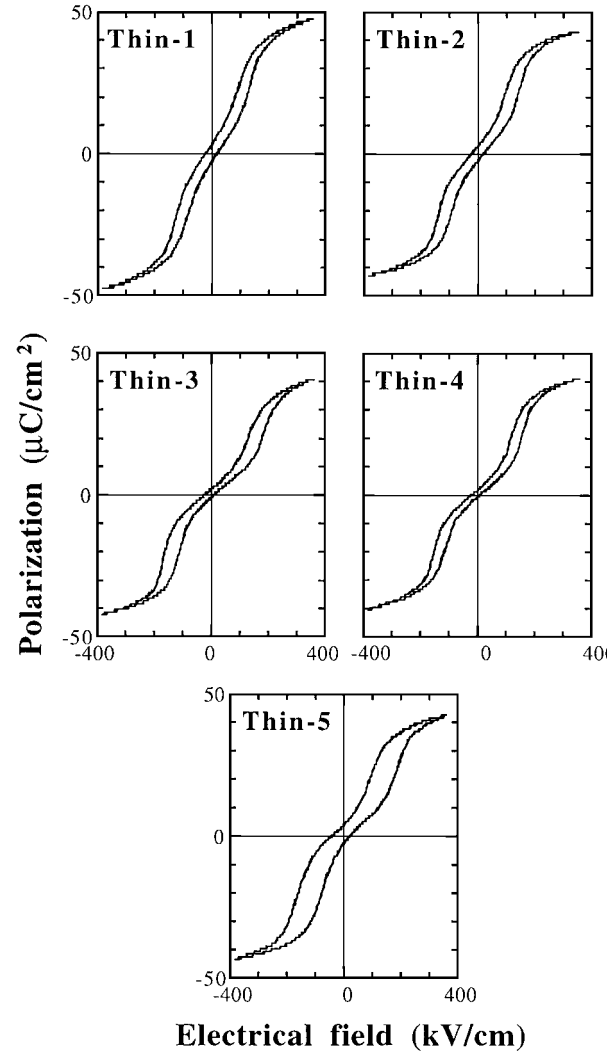

Figure 6 Hysteresis loops of the thin film samples in AFE tetragonal region.

lattice indices of the peaks are given according to the pseudocubic structure (the parent perovskite structure) no matter the compositions are located in tetragonal or orthorhombic region. The peaks with highest intensities are (111) and (200) for all the thin and thick films. It has been found that in the as-sintered bulk ceramics (random orientation), the strongest peak is (110), followed by (200) and (211), and the (111) peak is rather weak [15]. Hence these films can be considered as having (111) preferred orientation. Fig. 5 is the SEM picture of the Sample Thin-8 (PLZTS 2/85/2/13 – the abbreviation of the composition, same for the followings), which shows the presence of single phase and dense surface structure with the typical grain size of around 0.5 μm.

Samples from Thin-1 (PLZTS 2/66/9/25) to Thin-5 (PLZTS 2/85/7/8) have the compositions located in the AFE_T region, and their weak field dielectric properties are given in Table II. For the fixed Zr content (from Thin-1, PLZTS 2/66/9/25 to Thin-3, PLZTS 2/66/7/27), the dielectric constant decreases with the decrease of Ti content and the increase of Sn content. This is consistent to the results in bulk ceramics and can be attributed to the fact that the contribution of Ti^{4+} ions to the dielectric constant is significantly larger than that of the Sn^{4+} ions [6]. On the other hand, for the same Ti content, the dielectric constant of the films located in the higher Sn region (Thin-4, PLZTS 2/55/7/38) is much larger than that of the films located in the lower Sn region (Thin-3, PLZTS 2/66/7/27 and Thin-5, PLZTS 2/85/7/8). This is also similar to the results in bulk ceramics reported by Jaffe [16]. The field-induced hysteresis loops of these thin films are given in Fig. 6. The existence of double hysteresis loops confirms the antiferroelectric nature of these films. However, there is always some remanent polarization when the electrical field is removed, indicating the retention of the FE phase

in the films [9]. The switching fields of these films (and the following films in this study) are decided by the method proposed by ref. [8]. That is, the AFE-to-FE and the FE-to-AFE phase switching fields are determined as the intersections of the two lines representing the steepest and the flattest sections on the forward arm and backward arm, respectively, of the hysteresis loops. The phase switching fields of these thin films are also given in Table II. From Table II and Fig. 6 it can be seen that with further away from the AFE_T-$FE_{R(LT)}$ phase boundary and deeper into the AFE_T region (from Thin-1, PLZTS 2/66/9/25 to Thin-3, PLZTS 2/66/7/27), the phase switching fields increase and the values of remanent polarization decrease.

Samples from Thin-6 (PLZTS 2/65/4/31) to Thin-9 (PLZTS 2/90/2/8) are located in the AFE_O region of the phase diagram, and their weak field dielectric properties are given in Table II. For the same (or almost the same) Zr contents, the dielectric constant of the samples in the AFE_T region is larger than that of the samples in the AFE_O region (comparing Thin-3, PLZTS 2/66/7/27 to Thin-6, PLZTS 2/65/4/31 and Thin-5, PLZTS 2/85/7/8 to Thin-8, PLZTS 2/85/2/13). This variation is still consistent to bulk ceramics and also attributed to the fact that the contribution of Ti^{4+} ions to dielectric constant is significantly larger than that of the Sn^{4+} ions [6, 16]. Due to the limited dielectric strength, the room temperature hysteresis loops of the bulk ceramics located in the AFE_O region are seldom reported. However, the hysteresis loops of these thin films can be obtained and are given in Fig. 7 because the dielectric strength of thin films is much higher than that of bulk ceramics. It is interesting to note that all these thin films demonstrate zero remanent polarization after the electrical field is removed. The thin film in the AFE_O region with higher Sn content (Thin-6, PLZTS 2/65/4/31) displays

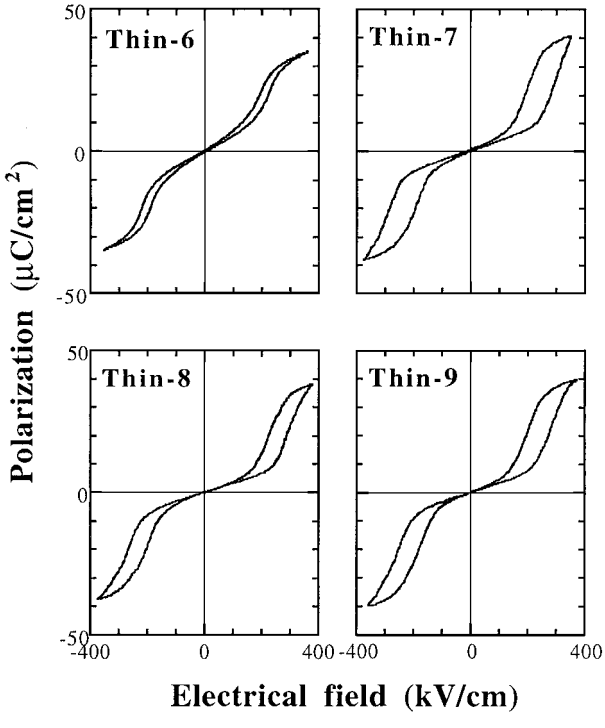

Figure 7 Hysteresis loops of the thin film samples in AFE orthorhombic region.

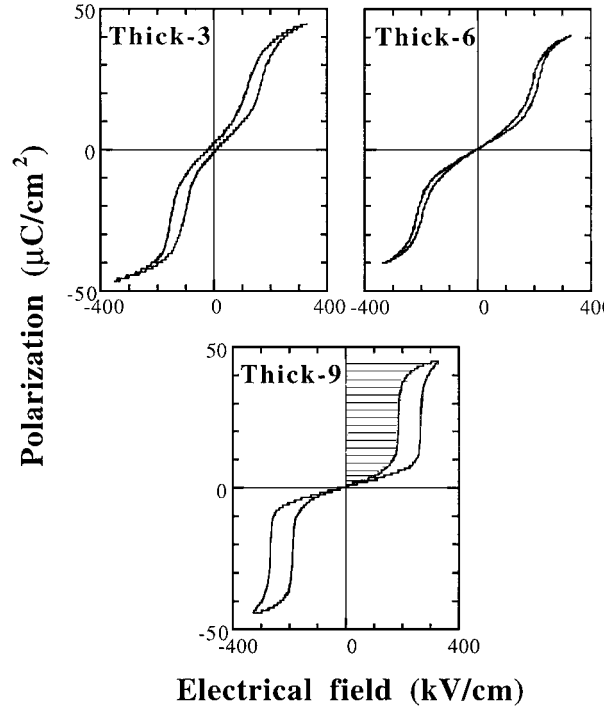

Figure 8 Hysteresis loops of the thick film samples.

a typical slanted hysteresis loop, which is suitable for analog electro-mechanical response applications. On the other hand, the thin films in the AFE_O region with higher Zr contents (Thin-7, PLZTS 2/90/5/5 to Thin-9, PLZTS 2/90/2/8) show typical square hysteresis loops with sharp phase switching, which are suitable for digital electro-mechanical response and energy-storage capacitor applications.

In order to clarify if the similar phenomena on composition dependence will occur for the thick films, several compositions are chosen to make thick films, with the thickness of about 5 μm (Samples Thick-3, Thick-6 and Thick-9). These thick films were prepared by the sol-gel method using acetic acid as solvent because we found it is difficult to prepare the thick films using 2-methoxyethanol as a solvent, as has been reported for PZT films [17, 18]. The electrical properties of these thick films are given in Fig. 8 and Table II. Comparing Fig. 8 to Figs 6 and 7, it can been seen that the variation of the shape of the hysteresis loops with compositions for the thick films is the same as that for thin films.

4. Discussion

The experimental results show that the dependence of weak field dielectric properties on compositions in AFE thin and thick films is similar to bulk ceramics but the high field properties (hysteresis loops) are quite different for films and bulk ceramics. Bulk ceramics can have square hysteresis loops with zero remanent polarization for most compositions in the AFE_T region [6], while all the films in the AFE_T region display definite remanent polarization and the phase switching is not very sharp. Zero remanent polarization can only be obtained for the films in the AFE_O region. Moreover, only the films in the AFE_O region with high Zr contents demonstrate typical square hysteresis loops with zero

remanent polarization. Because the phase switching or high field polarization is always accompanied with the change of dimensions (strains) for AFE materials, the switching should be obviously affected by the mechanical boundary conditions. Therefore, we propose that the phenomenon about the composition-dependent hysteresis loops for films is mostly due to their special mechanical constraint condition, that is, the residual stress effect caused by the thermal mismatch between the film and the substrate.

Although the stress effect in AFE films is seldom mentioned, it is well known that stress status can greatly change the domain configuration in $Pb(Zr,Ti)O_3$ (PZT) FE thin films. That is, the compressive stress will cause the films to have preferential c-domain orientation and the tensile stress will cause the films to have preferential a-domain orientation [19]. It is also known that when deposited on Si substrates, the PZT films with composition at morphotropic phase boundary (53/47 or 52/48) are under high tensile stress. This is because the thermal expansion coefficient of the high temperature paraelectric phase of the film ($6.7 \times 10^{-6}/^{\circ}C$) is larger than that of Si substrate ($2.6 \times 10^{-6}/^{\circ}C$) although the thermal expansion coefficient of the ferroelectric phase ($2.0 \times 10^{-6}/^{\circ}C$) is a little smaller [20]. We have calculated the thermal expansion coefficients of $PbZrO_3$ ceramics and another kind of AFE ceramics with the composition of $Pb_{0.97}La_{0.02}(Zr_{0.935}Ti_{0.04}Sn_{0.025})O_3$ from the reported thermal expansion curves [3, 21], and found the values are about $8 \times 10^{-6}/^{\circ}C$ for both the paraelectric phase and the AFE phase for these two kinds of ceramics [22]. For PZT system, Jaffe et al. suggested that the thermal expansion can be regarded qualitatively as an average of the normal expansion of $PbZrO_3$ and the strong thermal contraction of $PbTiO_3$ [23], hence the materials with higher Zr/Ti ratio should have larger thermal expansion coefficient. On the other hand, all the AFE ceramics have sharp volume contraction as transferred from the paraelectric phase to the AFE phase when cooled down because the primitive cell of the paraelectric phase is larger than that of the AFE phase [3]. However, the volume change of PZT (53/47) ceramics when transferred from the paraelectric phase to the FE phase is so small as to be almost undetectable [23]. Considering these results on bulk ceramics and the high Zr/Ti ratios (also high $Zr/(Ti + Sn)$ ratios) for the studied AFE thin and thick films, the thermal expansion coefficients of the AFE films should be larger than, or at least close to that of PZT (53/47) thin films. In addition, considering the large volume contraction for AFE materials from the paraelectric phase to the AFE phase, the AFE films should have larger dimension contraction comparing to PZT (53/47) thin films when cooled down. This means that the AFE films coated on Si substrates should be under high tensile stress when cooled from high temperature after annealing.

The primitive cell for the AFE materials in the AFE_T region and the AFE_O region is of the tetragonal structure (the complex orthorhombic cell in the AFE_O region is due to the antiparallel displacement of Pb^{2+} ions in the primitive, tetragonal cell [24]), with c/a less than 1 and the polar direction along [110] [24, 25]. When switched to the FE phase under high fields, the primitive cell becomes rhombohedral structure with the polarization along [111] direction. Because the α_{Rh} is very close to 90°, the a_{Rh} is slightly smaller than a_{Tet} but much larger than c_{Tet} [26, 27], in average the AFE ceramics (random oriented) will expand along all directions and have a large volume expansion when switched to the FE phase. Although the thin and thick films studied in this work have preferred (111) orientation (this can account for the high maximum polarization of the films), they still have random orientation in the film plane because they were not epitaxially grown. This means that they should expand in the film plane when switched to the FE phase under high electrical fields. Hence the high tensile stress should stabilize the FE phase with respect to the dimension variations, which is quite different from bulk ceramics which are generally under stress-free condition.

Because the films are prone to the FE phase under high tensile stress, the FE phase may be retained after electrical field removal if the free energy difference between the AFE phase and the FE phase is smaller. In general, for AFE materials the value of phase switching fields can be regarded as a measure of the free energy difference between the AFE phase and the FE phase [5]. The data in Table II show that the switching field values for the films in the AFE_T region are much smaller than that for the films in the AFE_O region. This indicates the free energy difference between the AFE phase and the FE phase for the films in the AFE_T region is much smaller than that for the films in the AFE_O region. Thus, it is possible that the tensile stress on the films in the AFE_T region is large enough to retain some FE phase after the electrical field is removed, which causes the existence of remanent polarization in the hysteresis loops. With compositions further away from the AFE_T-$FE_{R(LT)}$ phase boundary and deeper into the AFE_T region, the switching fields increase and the AFE phase becomes more stable, or the free energy difference between the AFE phase and the FE phase becomes larger. Thus the retained FE phase become less and the value of remanent polarization smaller. This is consistent with the experimental results for the samples from Thin-1 to Thin-3, as shown in Table II and Fig. 6. As the compositions enter the AFE_O region, the free energy difference between the AFE phase and the FE phase increases sharply, hence the tensile stress is not large enough to retain the FE phase after the electrical field is removed and zero remanent polarization can be obtained. On the other hand, for the compositions in the AFE_O region with high Zr contents, the tensile stress effect becomes much less comparing to the large free energy difference between the AFE phase and the FE phase. The hysteresis loops will mostly represent the intrinsic AFE-FE switching characteristics of the materials, leading to the fact that square hysteresis loops similar to bulk ceramics can be obtained, as shown by the results of the samples from Thin-7 to Thin-9 and Thick-9.

It should be mentioned that it is advantageous for energy-storage capacitor applications that square hysteresis loops with zero remanent polarization can be

TABLE III Energy storage density of some samples

Designation	Thin-7	Thin-8	Thin-9	Thick-9
Energy storage density (J/cm^3)	7.37	8.13	7.67	7.70

realized for the films in the AFE_O region with high Zr contents. This is because the energy storage density is equal to the area between the polarization axis and the back arm of the hysteresis loop [1], as the shaded area given in the Fig. 8 for the Thick-9 film. Thus, high switching fields and square hysteresis loops with zero remanent polarization can make the films have very high energy storage density. The energy storage density values have been calculated for the samples from Thin-7 to Thin-9 and Thick-9, and are listed in Table III. The energy storage density of these samples is larger than 7 J/cm^3, which will be very difficult for bulk ceramics to reach with the compositions in AFE_T region.

5. Summary

In this paper we have systematically studied the composition-dependent electrical properties of (Pb,La)(Zr,Ti,Sn)O_3 antiferroelectric-ferroelectric phase switching thin and thick films. The thin films with a thickness of about 0.4 μm and the thick films with a thickness of about 5 μm were deposited on Pt-buffered Si substrates by a sol-gel method using 2-methoxyethonal or acetic acid as a solvent. The results show that the dependence of low-field dielectric properties on compositions in the films are similar to that in bulk ceramics but the dependence of the high field properties (hysteresis loops) are quite different. While all the films with compositions in the AFE_T region in the phase diagram display the existence of remanent polarization in the hysteresis loops, zero remanent polarization can be obtained for the films with compositions in the AFE_O region. This is because the films are under high tensile stress after annealing, which enhances the stability of the FE phase and leads to the retention of the FE phase for the films in the AFE_T region because of their relatively small free energy difference between the AFE phase and the FE phase. Only in the AFE_O region and with high Zr contents, can the films be obtained with typical square hysteresis loops and sharp phase switching, which, for most part, represents the intrinsic AFE-FE switching behavior of the materials. The films in the AFE_O region and with high Zr contents can have very high energy storage density, thus they are very promising for high energy-storage capacitor applications such as decoupling capacitors in advanced multichip modules.

Acknowledgement

The authors are grateful to the Office of Naval Research for the financial support on the thin film work and the Charles Stark Draper Laboratory (Boston, MA) for the financial support on the thick film work.

References

1. B. JAFFE, *Proc. IRE* **49** (1961) 1264.
2. D. BERLINCOURT, H. H. A. KRUEGER and B. JAFFE, *J. Phys. Chem. Solids* **25** (1964) 659.
3. D. BERLINCOURT, *IEEE Trans. Sonics Ultrason.* **13** (1966) 116.
4. K. UCHINO and S. NOMURA, *Ferroelectrics* **50** (1983) 517.
5. W. Y. PAN, C. Q. DAM, Q. M. ZHANG and L. E. CROSS, *J. Appl. Phys.* **66** (1989) 6014.
6. K. MARKOWSKI, S. E. PARK, S. YOSHIKAWA and L. E. CROSS, *J. Am. Ceram. Soc.* **79** (1996) 3297.
7. Y. AKIYAMA, S. KIMURA and I. FUJIMURA, *Jpn. J. Appl. Phys.* **32** (1993) 4154.
8. K. G. BROOKS, J. CHEN, K. R. UDAYAKUMAR and L. E. CROSS, *J. Appl. Phys.* **75** (1994) 1699.
9. S. S. SENGUPTA, D. ROBERTS, J. F. LI, M. C. KIM and D. A. PAYNE, *ibid.* **78** (1995) 1171.
10. C. J. GASKEY, K. R. UDAYAKUMAR, H. D. CHEN and L. E. CROSS, *J. Mater. Res.* **10** (1995) 2764.
11. B. XU, N. G. PAI and L. E. CROSS, *Mater. Lett.* **35** (1998) 157.
12. B. XU, L. E. CROSS and D. RAVICHANDRAN, *J. Am. Ceram. Soc.* **82** (1999) 306.
13. B. XU, N. G. PAI, Q.-M. WANG and L. E. CROSS, *Integrated Ferroelectrics* **22** (1998) 545.
14. B. XU, P. MOSES, N. G. PAI and L. E. CROSS, *Appl. Phys. Lett.* **72** (1998) 593.
15. S.-E. PARK, M.-J. PAN, K. MARKOWSKI, S. YOSHIKAWA and L. E. CROSS, *J. Appl. Phys.* **82** (1997) 1798.
16. B. JAFFE, "Research on antiferroelectric materials," Cleavite Report to U.S. Army, Project No. 302490, 1962.
17. B. A. TUTTLE and R. W. SCHWARTZ, *MRS Bulletin* **21**(6) (1996) 49.
18. H. D. CHEN, K. R. UDAYAKUMAR, C. J. GASKEY and L. E. CROSS, *J. Am. Ceram. Soc.* **79** (1995) 2189.
19. B. A. TUTTLE, T. J. GARINO, J. A. VOIGT, T. J. HEADLEY, D. DIMOS and M. O. EATOUGH, in "Science and Technology of Electroceramic Thin Films," edited by O. Auciello and R. Ramesh (Kluwer Academic Publishers, Netherlands, 1995) p. 117.
20. B. A. TUTTLE, J. A. VOIGT, T. J. GARINO, D. C. GOODNOW, R. W. SCHWARTZ, D. L. LAMPPA, T. J. HEADLY and M. O. EATOUGH, in Proceedings of the 1992 IEEE 8th International Symposium on Applications of Ferroelectrics (The Institute of Electrical and Electronic Engineers, Piscataway, NJ, USA, 1992) p. 344.
21. E. SAWAGUSHI, G. SHIRANE and Y. TAKAGI, *J. Phys. Soc. Jap.* **6** (1951) 333.
22. B. XU, Y. YE, Q.-M. WANG, and L. E. CROSS, *J. Appl. Phys.* **85** (1999) 3753.
23. B. JAFFE, W. R. COOK and H. JAFFE, "Piezoelectric Ceramics" (Academic Press, Ohio, USA, 1971) p. 167.
24. E. SAWAGUCHI, H. MANIWA and S. HOSHINO, *Phys. Rev.* **83** (1951) 1078.
25. J. S. SPECK, M. D. GRAEF, A. P. WILKINSON, A. K. CHEETHAM and D. R. CLARKE, *J. Appl. Phys.* **73** (1993) 7261.
26. L. SHEVANOV, M. KUSNETSOV and A. STERNBERG, *ibid.* **76** (1994) 4301.
27. C. T. BLUE, C. T. HICKS, S.-E. PARK, S. YOSHIKAWA and L. E. CROSS, *Appl. Phys. Lett.* **68** (1996) 2942.

Received 9 February 1999
and accepted 2 May 2000